

# Anisotropic optical band gap of (102)- and (002)-oriented films of red $\text{HgI}_2$

Pankaj Tyagi and A. G. Vedeshwar\*

*Thin Film Lab, Department of Physics and Astrophysics, University of Delhi, Delhi-110 007, India*

(Received 7 November 2000; revised manuscript received 22 February 2001; published 6 June 2001)

The thermally evaporated stoichiometric films of  $\text{HgI}_2$  show a preferred orientation of (102) and (002) parallel to substrate plane for film thicknesses below and above 1450 nm, respectively. The band gap determined by optical absorption shows the anisotropic nature of the two orientations with an anisotropic ratio  $E_{g(102)}/E_{g(002)} = 0.86$ . The change in band gap with film thickness in either orientation is attributed to the residual stress in the film. An increase in the band gap with residual stress is observed for the (102) orientation as opposed to a decreasing band gap with stress for the (002) orientation. The annealing experiment carried out on the (102)-oriented film shows a switch over to the (002) orientation at 110 °C. The results of the annealing experiment support well the results of thickness dependence, viz., the anisotropic nature of the band gap at two orientations and the residual stress-induced band gap change.

DOI: 10.1103/PhysRevB.63.245315

PACS number(s): 68.55.Jk, 78.20.Ci, 78.66.Li, 81.15.Ef

## I. INTRODUCTION

Mercury iodide ( $\text{HgI}_2$ ) is a layered semiconductor better known as a radiation (x rays and  $\gamma$  rays) detector material in its red, tetragonal form.<sup>1–8</sup> It can also exist in orthorhombic and hexagonal structures. However, the tetragonal form has been studied quite extensively because of its application as a radiation detector. Most of the studies concentrated on optical properties<sup>9–19</sup> such as absorption, reflectivity, and photoluminescence. There have been theoretical calculations of the band structure explaining most of the observed optical properties.<sup>20–23</sup> There are few reports concerning the physical properties of  $\text{HgI}_2$  such as photoconductivity, photoluminescence, and thermally stimulated current regarding its quality for application as a radiation detector.<sup>24–26</sup> The anisotropic nature of optical properties, perpendicular and parallel to the  $c$  axis, has been demonstrated both theoretically<sup>21–23</sup> and experimentally.<sup>10–14,19</sup> In the tetragonal lattice each mercury atom is tetrahedrally bonded to four iodine atoms, and each iodine atom has only two bonds. This arrangement makes the structure to be intermediate between the layer structure and fully tetrahedrally bonded structure. Therefore, the tetragonal structure of  $\text{HgI}_2$  is also regarded as a tetrahedral defect structure. The influence of the defect structure due to the iodine deficiency has also been studied in relation to detector quality.<sup>26</sup> A phase transformation from tetragonal to orthorhombic has also been observed at 126 °C.<sup>11</sup> Both theoretical and experimental studies show that  $\text{HgI}_2$  is a direct band gap (2.13 eV) material except only one report,<sup>16</sup> which shows both direct and indirect band gaps. Almost all the studies have been done on single crystal samples grown by different techniques. Surprisingly, there are very few reports on thin films of  $\text{HgI}_2$ .<sup>11,27</sup> They are also not adequately informative and systematic regarding basic thin film properties. This could be due to the very high vapor pressure of  $\text{HgI}_2$  leading to nonformation of films at very low pressures. Since the thin film form of any material is quite advantageous in many applications, we thought it necessary and worthwhile to investigate systematically the basic physical properties of  $\text{HgI}_2$  in thin film form.

## II. EXPERIMENTAL DETAILS

The thin films of  $\text{HgI}_2$  were grown on glass substrates (2 cm  $\times$  6 cm) at room temperature by thermal evaporation using a molybdenum boat. The starting material was a high purity analar grade powder that was palletized for evaporation. All the films used in this study were grown at the vacuum of  $10^{-5}$  Torr. At higher pressures films were non-uniform and sticking was poor. The main problem encountered in the film preparation is due to the high vapor pressure of  $\text{HgI}_2$ . Therefore, it is quite difficult to get films thinner than 900 nm and to control the film thickness at the desired value. We have kept the deposition rate quite slow, of about 3–5 nm/sec. We could grow uniform good quality films only in the thickness range 900–2100 nm using these optimum conditions. The thicker films were not useful in optical absorption studies as their absorption was very high in the optical region of interest. We could not get any film for a substrate temperature higher than the room temperature. The films were whitish translucent immediately after the growth and turned to a reddish orange color similar to the starting material in an hour or so. The film thickness was monitored during the growth by a quartz crystal thickness monitor and was subsequently determined by a Dektak IIA surface profiler. Small pieces of 5 mm  $\times$  5 mm were cut for various analyses so as to carry out different analyses on the same film. The structural studies of the films were carried out by x-ray diffraction (PHILLIPS X-Pert model, 1830). The film composition was found to be stoichiometric as determined by EDAX (JEOL-840). The morphology of the films was studied by scanning electron microscopy (SEM) (JEOL, 840). The optical absorption measurements were carried out in ultraviolet-visible region using a (Shimadzu UV, 260) spectrophotometer.

## III. RESULTS AND DISCUSSIONS

The structural studies were carried out on various films in the thickness range 900–2100 nm. All the observed lines in x-ray diffraction data match very well with ASTM Card No. 21-1157 for  $\text{HgI}_2$  crystal confirming the stoichiometric com-

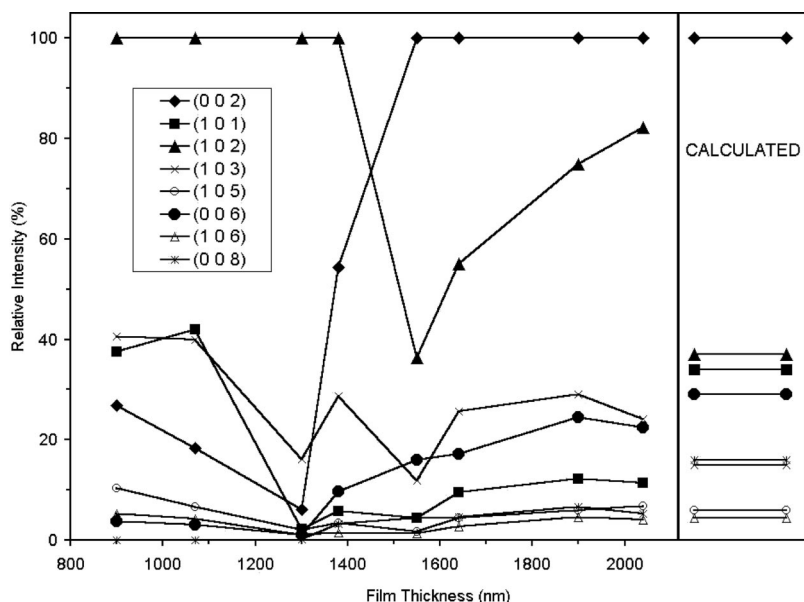


FIG. 1. Relative intensities of x-ray diffraction peaks of  $\text{HgI}_2$  films as a function of film thickness. The calculated relative intensities for the observed diffraction peaks are shown at the right side.

position of the films as determined by energy-dispersive x-ray analysis (EDAX) and the tetragonal structure with  $a = b = 0.437$  nm and  $c = 1.244$  nm. The diffraction data show only  $(10l)$  and  $(00l)$  reflections in all the films studied. However, the relative intensities of these reflections show film thickness dependence as shown in Fig. 1. On the right of Fig. 1 we have also shown the calculated relative intensity for these reflections for comparison. The diffracted intensities were calculated following a well known standard procedure<sup>28</sup> that includes the structure factor for the desired reflecting plane. There are two Hg atoms and four I atoms in a unit cell and their atomic coordinates were taken from reference of Turner and Harmon,<sup>20</sup> which has the same cell dimensions as given above. The calculated intensity does not depend on the film thickness and is valid only for a sample containing completely randomly oriented crystallites. When a disagreement exists between observed and calculated intensities, as in the present case (Fig. 1), preferred orientation should be the first possible cause to be suspected.<sup>28</sup> Therefore, from Fig. 1 we can infer a preferred growth of grain orientation with the  $(102)$  plane parallel to substrate plane for films of thickness  $< 1450$  nm and with the  $(002)$  plane parallel to the substrate plane for a film thickness  $> 1450$  nm. This fact is further confirmed by the grain morphology (SEM) of films of different orientations as shown in Fig. 2.

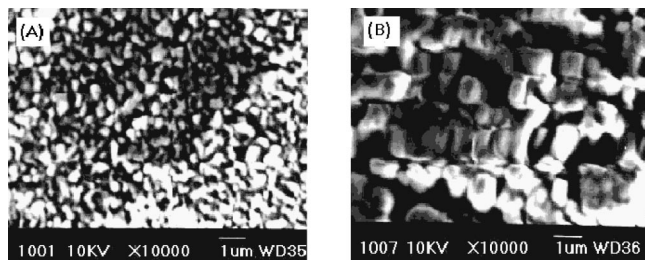


FIG. 2. The morphology as seen by SEM for an (A)  $(102)$ -oriented 1300 nm thick and (B)  $(002)$ -oriented 1550 nm thick  $\text{HgI}_2$  film.

All  $(00l)$  planes are parallel and show almost a similar trend in thickness-dependent intensities. The other important observation in Fig. 1 is the increasing intensities of other reflections in opposite directions from the vicinity of 1450 nm film thickness. The increasing presence of other nonparallel planes could cause a nonuniform strain in the film due to residual stress. The nonuniform strain in the film can be estimated qualitatively by the slope of the peak full width at half maximum (FWHM)  $\Delta(2\theta)$  versus  $\sin(\theta)$  plot. However, in oriented films the appropriate quantity would be the strain produced  $\Delta d_{hkl}/d_{hkl}$  on the oriented plane  $(hkl)$ , which can be estimated relatively by the  $d$  spacing. If the quantity  $\Delta d_{hkl}/d_{hkl}$  [which is also proportional to  $\Delta(2\theta)$ ] is multiplied by the elastic constant of the material, the residual stress along the plane can be obtained. We have found from the diffraction data that the strain increases with decreasing thickness below 1450 nm and increases with increasing thickness above 1450 nm as shown in Fig. 3. We can see that the magnitude of increase in strain on either side of film thickness 1450 nm is different and almost correlates with the

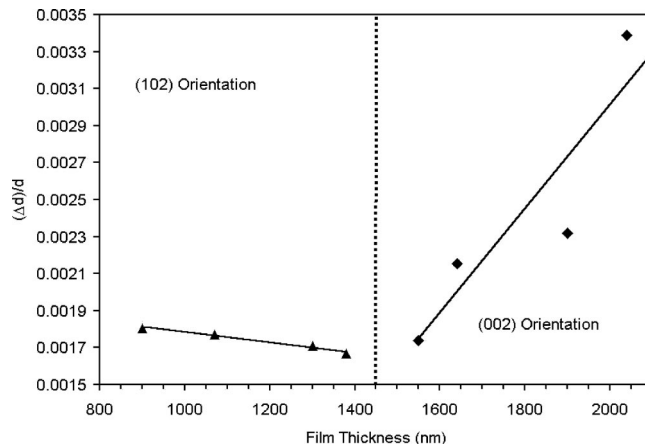


FIG. 3. The residual stress parameter  $\Delta d_{hkl}/d_{hkl}$  as a function of  $\text{HgI}_2$  film thickness for the two crystallite orientations.

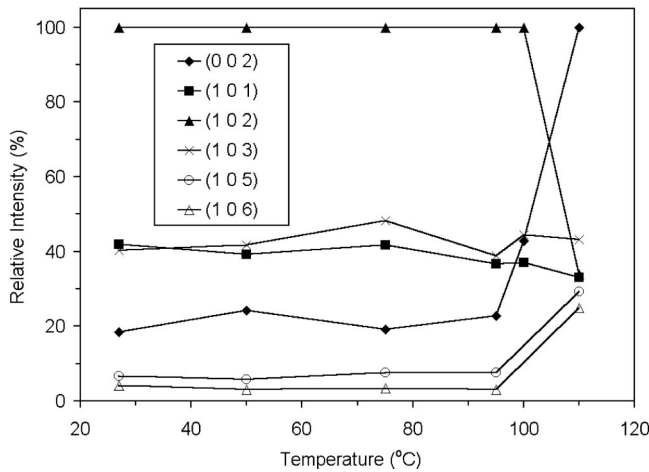


FIG. 4. Relative intensities of x-ray diffraction peaks of a 1070 nm thick  $\text{HgI}_2$  film as a function of annealing temperature.

increase in intensity of (102) on the left and of (002) on the right from the vicinity of 1450 nm film thickness in Fig. 1. Since we could not find the elastic constant for  $\text{HgI}_2$ , we could not estimate the stress quantitatively. Therefore, the residual stress also should behave in the same manner as the strain qualitatively within the elastic limit.

We have also tried to study the effect of annealing on the orientation of the films. We have annealed  $\text{HgI}_2$  films in air for a very short duration ( $\sim 30$  sec) at various temperatures up to  $110^\circ\text{C}$ . Above  $110^\circ\text{C}$ , the film vanishes on annealing even for few seconds. Figure 4 shows the intensity profile of diffraction peaks as a function of annealing temperature of a (102)-oriented film of thickness 1070 nm. As can be seen from the figure, the (102) orientation switches to (002) orientation at  $110^\circ\text{C}$ . It can be noted that there is only a change in the relative intensities of the oriented planes and no change in  $d$  spacing. Therefore, it is not a structural phase transformation. A tetragonal to orthorhombic phase transition is known to take place in  $\text{HgI}_2$  at about  $126^\circ\text{C}$ .

The optical absorption of the films in the UV-visible region was recorded using the double-beam ratio recording technique in transmission mode. The absorption coefficient  $\alpha$  was calculated using measured absorbance as a function of incident photon energy using the relation

$$\alpha = \frac{2.303A}{t}, \quad (1)$$

where  $A$  is the absorbance and  $t$  is the film thickness, neglecting the reflection coefficient, which is negligible and insignificant near the absorption edge. The absorption data are shown for some film thicknesses in Fig. 5. The absorption coefficient at energies lower than the interband absorption edge does not show constancy with thickness as can be expected in the general case according to Eq. (1), since absorbance is a function of film thickness. The explicit dependence of  $\alpha$  on film thickness for a particular energy (2.08 eV) less than the band edge is displayed in Fig. 6. The behavior, even though looking strange, seems to be consistent with x-ray diffraction observations. The vertical line in the

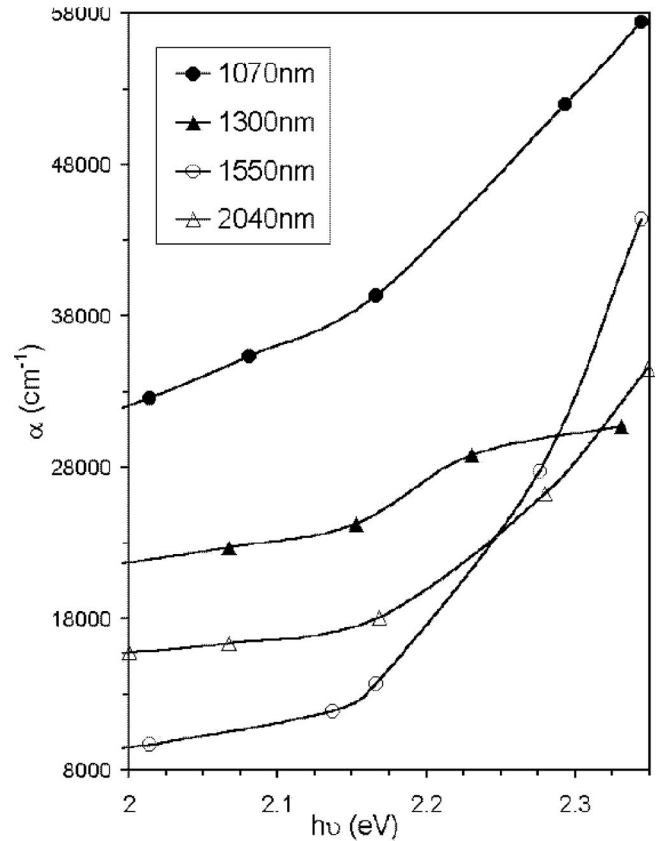


FIG. 5. The optical absorption of  $\text{HgI}_2$  films as a function of incident photon energy for different film thicknesses. The upper two curves are for (102)-oriented films and the lower two curves are for (002)-oriented films.

figure at 1450 nm separates the two regions of crystallite orientations. On either side, the absorption coefficient increases, which is quite similar to the residual stress behavior except for the slope. It indicates a lesser sensitivity of  $\alpha$  on residual stress for the (002) orientation and a greater sensitivity for the (102) orientation. The increase in  $\alpha$  with externally applied stress has been observed in single crystal  $\text{HgI}_2$ .<sup>18</sup> Therefore, the thickness dependence of  $\alpha$  on either

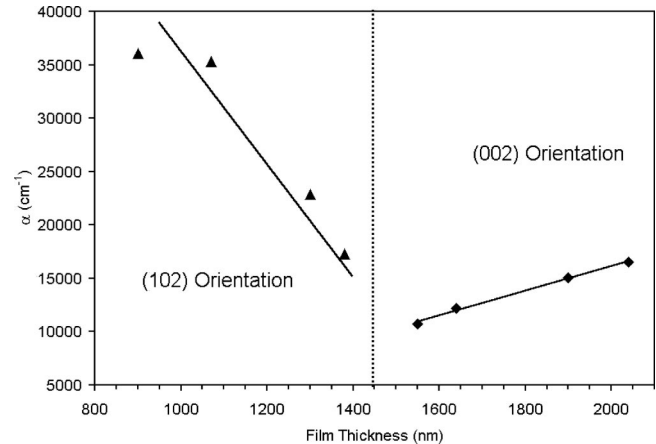


FIG. 6. The dependence of the absorption coefficient (at 2.08 eV) on  $\text{HgI}_2$  film thickness for the two crystallite orientations.

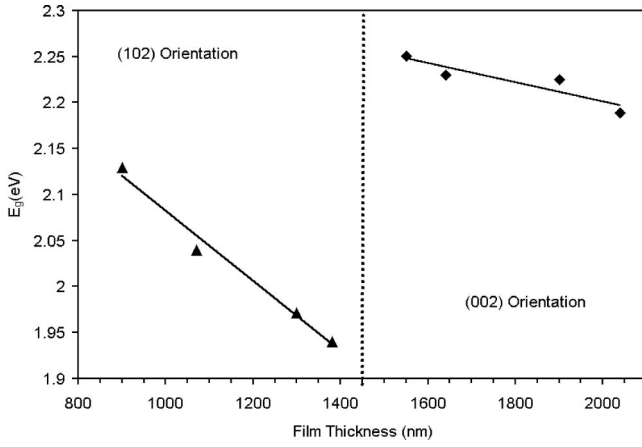


FIG. 7. The thickness dependence of optical band gaps  $E_{g(102)}$  and  $E_{g(002)}$  of  $\text{HgI}_2$  films for the two crystallite orientations.

side of the crystallite orientation is very much consistent with structural studies. As can be seen from the figure, the absorption from the (102) plane is higher than that of the (002) plane. This is quite consistent due to the fact that there are fewer atoms on (002) than on (102) as can be seen from the crystal structure of  $\text{HgI}_2$ .<sup>20</sup> Since the optical absorption measurements were carried out in the transmission mode at normal incidence, we can regard the data as perpendicular to the (102) and (002) planes for film thicknesses smaller and greater than 1450 nm, respectively. Since all (00 $l$ ) planes are parallel to the basal plane (001), the alignment of the  $c$  axis is perpendicular to the substrate plane in (002)-oriented films. Therefore, the optical data can be treated as parallel to  $c$  axis in this case. In the other case it is simply for the perpendicular direction to the (102) plane.

The optical band gap of the material can be determined, usually from the intercept of the linear part of the  $(\alpha h\nu)^{1/n}$  versus  $h\nu$  plot in the region of interband absorption. For the allowed direct band gap material  $n = 1/2$  and the plot shows a single linear portion. For the allowed indirect transition  $n = 2$  and the plot shows two linear portions yielding two intercepts  $(E_g + E_p)$  and  $(E_g - E_p)$ , where  $E_p$  is the phonon energy assisting the transition. We have tried both the possibilities. We have obtained best fit for  $n = 1/2$  with a correlation factor of least square fitting better than 0.96. The fitting with  $n = 2$  shows a poor correlation factor of less than 0.8 and yields an incomprehensibly high phonon energy. Therefore, the band gap is determined to be direct for  $\text{HgI}_2$  films as has been already established both experimentally and theoretically. The band gap as a function of film thickness is shown in Fig. 7 for the two crystallite orientations. A vertical line is shown in the figure to highlight (102)-oriented films on the left and (002)-oriented films on the right. Therefore, as discussed above we can regard the band gap on the left as  $E_{g(102)}$  in the direction perpendicular to the (102) plane and on the right as  $E_{g(002)} = E_{g\parallel}$  (parallel to the  $c$  axis of tetragonal lattice of  $\text{HgI}_2$ ). On either side of the separation, the band gap changes with thickness in moving away from the separation line. The band gap decreases with thickness in both orientations with different slopes. As we have seen earlier in the correlation of  $\alpha$  with residual stress as a function

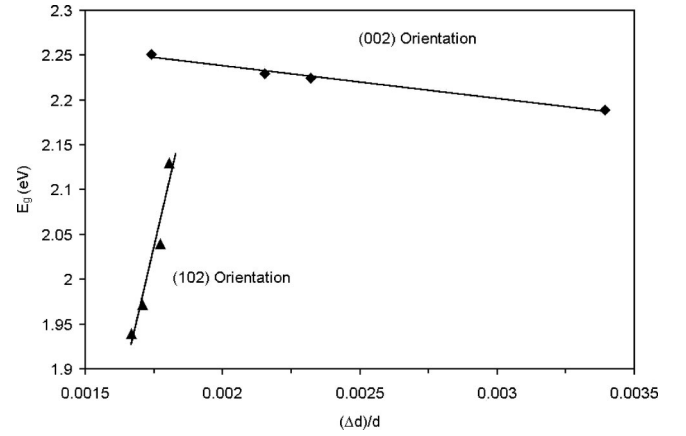


FIG. 8. The variation of  $E_{g(102)}$  and  $E_{g(002)}$  with the residual stress parameter  $\Delta d_{hkl}/d_{hkl}$  for (102)- and (002)-oriented  $\text{HgI}_2$  films, respectively.

of thickness from Figs. 3 and 6, it is quite reasonable to correlate the change in  $E_g$  with  $\Delta d/d$ . Comparing Figs. 3 and 7, we can see a stronger effect of residual stress in changing  $E_{g(102)}$  and a relatively weaker effect in changing  $E_{g(002)}$ . Also, the residual stress seems to increase  $E_{g(102)}$  while it decreases  $E_{g(002)}$ . There is only one report regarding the effect of externally applied stress on  $E_g$  of  $\text{HgI}_2$  single crystal that is qualitative in nature.<sup>18</sup> A decrease of 0.034 eV has been reported at higher pressure. The magnitude of pressure is not known. In the present study also we have observed a decrease of 0.062 eV in  $E_{g(002)}$  at a maximum increase of 0.0017 in  $\Delta d_{(002)}/d_{(002)}$ . The knowledge of the elastic constant would help us to quantify the magnitude of internal stress in the film. On the other hand, a large increase of 0.19 eV has been observed in  $E_{g(102)}$  at the maximum increase of 0.00019 in  $\Delta d_{(102)}/d_{(102)}$ . The variation of band gap with residual stress in both orientations is illustrated explicitly in Fig. 8. As discussed above,  $E_{g(102)}$  is much more sensitive than  $E_{g(002)}$  to a change in  $\Delta d/d$ . Both  $E_{g(102)}$  and  $E_{g(002)}$  vary linearly with  $\Delta d/d$  in opposite directions with a different magnitude of slope of 1306 eV/ $(\Delta d/d)$  and  $-36$  eV/ $(\Delta d/d)$ , respectively in the limited region of experimentally determined residual stress. This kind of anisotropy in the band structure can be attributed to the basic structural arrangements of Hg and I atoms in the tetragonal unit cell. The large ratio of lattice parameters  $c/a = 2.86$  makes the structure fairly open with a small packing fraction. Therefore, the effect of pressure either internal or external could cause a change in the nearest neighbor distance of atoms in the unit cell anisotropically in different directions modifying the band structure. Therefore we believe the present results could be quite useful and informative regarding the band structure of  $\text{HgI}_2$ . A theoretical investigation of band structure for changing interatomic distances in a perpendicular direction to (102) and (002) planes could verify these results. The anisotropy perpendicular and parallel to the  $c$  axis in single crystals has been observed in the measurements of optical reflectivity,<sup>11,14</sup> excitonic absorption<sup>12</sup> [anisotropic ratios in refractive index  $n_{\perp}/n_{\parallel} = 1.07$ , dielectric constant  $\epsilon_{\perp}/\epsilon_{\parallel} = 1.15$ , electron drift mobility  $\mu_{D\perp}/\mu_{D\parallel}$

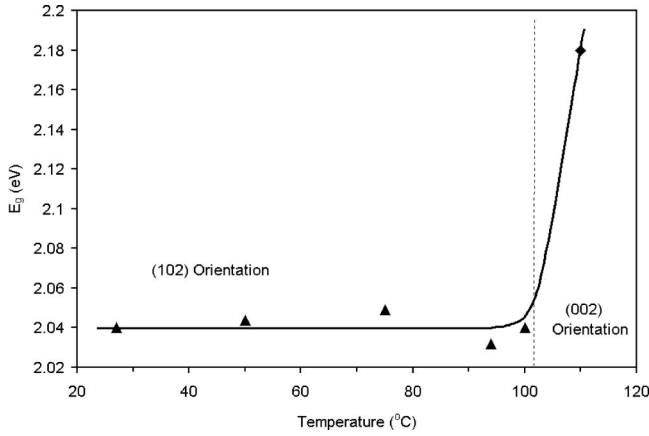


FIG. 9. The dependence of the optical band gap of a 1070 nm thick  $\text{HgI}_2$  film on annealing temperature. The different crystallite orientations are specified on the basis of x-ray diffraction data of Fig. 4.

$=1.4$ , and the electron effective mass  $m_{e\perp}/m_{e\parallel}=1.2$  (Refs. 12, 13 and 29)], cyclotron resonance,<sup>13</sup> and dielectric response.<sup>19</sup> The theoretical calculation also reveals the anisotropic nature of carrier effective mass and mobility.<sup>21</sup> The only report, by Yao, Johs, and James,<sup>19</sup> shows the anisotropic edge  $E_{g\perp}=2.25$  eV and  $E_{g\parallel}=2.43$  eV with  $E_{g\perp}-E_{g\parallel}=-0.18$  eV and  $E_{g\perp}/E_{g\parallel}=0.93$  by the measurements of anisotropic dielectric functions. The anisotropic band gaps were determined by  $\epsilon_2$  versus  $h\nu$  plots by taking the value of  $h\nu$  at which  $\epsilon_2$  goes to zero. The anisotropic band gaps in the present study having the lowest residual stress  $E_{g(102)}=1.94$  eV and  $E_{g(002)}=2.25$  eV with  $E_{g(102)}-E_{g(002)}=-0.31$  eV and  $E_{g(102)}/E_{g(002)}=0.86$  are not in a direction perpendicular to each other as opposed to the case of the  $c$  axis parallel and perpendicular data. However, the comparison is still good. As mentioned earlier we have  $E_{g(002)}=E_{g\parallel}=2.25$  eV from the present study having some residual stress can be extrapolated from Fig. 8 to get  $E_{g\parallel}=2.40$  eV at zero residual stress, which compares very well with the reported  $E_{g\parallel}=2.43$  eV.<sup>19</sup> Also, the average of  $E_{g(102)}$  and  $E_{g(002)}$  equal to 2.1 eV agrees quite well with the most established value of 2.13 eV for single crystals.

In our annealing experiment on a (102)-oriented film, we have seen a jump in the band gap value at 110 °C as shown in Fig. 9. In this figure also we have shown a vertical line to differentiate between the (102) orientation on the left and the (002) orientation on the right as has been revealed by x-ray

diffraction studies shown in Fig. 4.  $E_{g(002)}=2.18$  eV (at 110 °C) is quite comparable with  $E_{g(002)}=2.19$  eV of Fig. 7 with  $\Delta d/d=0.0034$ . The amount of residual stress present in the annealed film in the (002) orientation was determined to be of comparable magnitude [ $\Delta d_{(002)}/d_{(002)}=0.0038$ ], which could be due to the increased presence of the (105) and (106) planes at this annealing temperature, as can be compared in Figs. 1 and 4. The change in  $\Delta d_{(102)}/d_{(102)}$  is practically negligible up to an annealing temperature of 100 °C consistent with the observed behavior of  $E_{g(102)}$  with annealing temperature. This is quite understandable by the almost constant intensities of other reflecting planes up to 100 °C as can be seen from Fig. 4. Therefore, the optical band gap determined from the annealing experiment is quite consistent with structural studies as well as the thickness dependence data.

#### IV. CONCLUSIONS

The thin film growth of  $\text{HgI}_2$  is studied systematically using structural, compositional, morphological, and optical absorption analyses. All these analyses are consistent with the preferred (102) and (002) orientations parallel to the substrate plane for film thicknesses below and above 1450 nm, respectively. The results of the annealing experiment supports quite well the observations of thickness dependence, viz., the anisotropic nature of the band gap at the two orientations and a residual stress-induced band gap change. The anisotropic ratio  $E_{g(102)}/E_{g(002)}=0.86$  observed in the present study compares quite well with the only reported band gap anisotropic ratio  $E_{g\perp}/E_{g\parallel}=0.93$ . An increase in band gap with residual stress has been observed along the (102) orientation in opposition to the decrease in band gap with stress for the (002) orientation. This kind of anisotropy in the stress-induced change in band gap is being pursued theoretically using band structure and crystallographic data as an ongoing investigation.

#### ACKNOWLEDGMENTS

We would like to thank Dr. P. Arun, Vinod Kumar Paliwal, Namit Mahajan, and Hina for their helpful discussions and Mr. P. C. Padmakshan, Department of Geology, University of Delhi, for carrying out x-ray diffraction measurements. The help of Dr. N. C. Mehra, USIC, Delhi University in the measurements of EDAX and SEM is gratefully acknowledged.

\*Electronic address: agni@physics.du.ac.in

<sup>1</sup>W.R. Willing, Nucl. Instrum. Methods **96**, 615 (1971).

<sup>2</sup>S.P. Swierkowski, G.A. Armantrout, and R. Wichne, IEEE Trans. Nucl. Sci. **NS-21**, 302 (1974).

<sup>3</sup>J.P. Ponpon, R. Stuck, P. Siffert, B. Meyer, and C. Schwab, IEEE Trans. Nucl. Sci. **22**, 182 (1975).

<sup>4</sup>R.C. Whited and M. Schieber, Nucl. Instrum. Methods **162**, 119 (1979).

<sup>5</sup>A.J. Dabrowski, W.M. Szymczyk, J.S. Iwanczyk, J.H. Kusmiss, W. Drummond, and L. Ames, Nucl. Instrum. Methods Phys.

Res. **213**, 89 (1983).

<sup>6</sup>D. Wong, T.E. Schlesinger, R.B. James, C. Ortale, L. van den Berg, and W.F. Schnepple, J. Appl. Phys. **64**, 2049 (1988).

<sup>7</sup>V. Gerrish and L. van den Berg, Nucl. Instrum. Methods Phys. Res. A **294**, 41 (1990).

<sup>8</sup>A. Burger, S.H. Morgon, E. Silberman, D. Nason, and A.Y. Cheng, Nucl. Instrum. Methods Phys. Res. A **322**, 427 (1992).

<sup>9</sup>R.H. Bube, Phys. Rev. **106**, 703 (1957).

<sup>10</sup>B.V. Novikov and M.M. Pimonenko, Fiz. Tekh. Poluprovodn. **4**, 2077 (1970); [Sov. Phys. Semicond. **4**, 1785 (1971)]; **6**, 771

- (1972) [ **6**, 671 (1972)].
- <sup>11</sup>K. Kanzaki and I. Imai, J. Phys. Soc. Jpn. **32**, 1003 (1972).
  - <sup>12</sup>A. Anedda, F. Raga, E. Grilli, and M. Guzzi, Nuovo Cimento Soc. Ital. Fis., B **38**, 439 (1977).
  - <sup>13</sup>P.D. Bloch, J.W. Hodby, C. Schwab, and D.W. Stacey, J. Phys. C **11**, 2579 (1978).
  - <sup>14</sup>A. Anedda, E. Grilli, M. Guzzi, F. Raga, and A. Serpi, Solid State Commun. **39**, 1121 (1981).
  - <sup>15</sup>J. Bornstein, and R.H. Bube, J. Appl. Phys. **61**, 2676 (1987).
  - <sup>16</sup>E. Lopez-Cruz, J. Appl. Phys. **65**, 874 (1989).
  - <sup>17</sup>A. Burger and D. Nason, J. Appl. Phys. **71**, 2717 (1992).
  - <sup>18</sup>M. Gonzalez and A. Ibarra, Phys. Rev. B **51**, 13 786 (1995).
  - <sup>19</sup>H. Yao, B. Johs, and R.B. James, Phys. Rev. B **56**, 9414 (1997).
  - <sup>20</sup>D.E. Turner and B.N. Harmon, Phys. Rev. B **40**, 10 516 (1989).
  - <sup>21</sup>Y.C. Chang and R.B. James, Phys. Rev. B **46**, 15 040 (1992).
  - <sup>22</sup>R. Ahuja, O. Eriksson, B. Johansson, S. Auluck, and J.M. Wills, Phys. Rev. B **54**, 10 419 (1996).
  - <sup>23</sup>A.K. Solanki, A. Kashyap, T. Nautiyal, S. Auluck, and M.A. Khan, Phys. Rev. B **55**, 9215 (1997).
  - <sup>24</sup>C.D. Blasi, S. Gulassini, C. Manfredotti, G. Micocci, L. Ruggiero, and A. Tepore, Nucl. Instrum. Methods **150**, 103 (1978).
  - <sup>25</sup>J.C. Muller, A. Friant, and P. Siffert, Nucl. Instrum. Methods **150**, 97 (1978).
  - <sup>26</sup>X.J. Bao, T.E. Schlesinger, R.B. James, R.H. Stulen, C. Ortale, and A.Y. Cheng, J. Appl. Phys. **68**, 86 (1990).
  - <sup>27</sup>A.B. Epstein, R.J. Ebert, and C. Coleman, Thin Solid Films **151**, 429 (1987).
  - <sup>28</sup>B.D. Cullity, *Elements of X-Ray Diffraction* 2nd ed. (Addison-Wesley, Reading, 1978), pp. 107–143.
  - <sup>29</sup>I.Ch. Schluter and M. Schluter, Phys. Rev. B **9**, 1652 (1974).